Human Molecular Genetics, 1999, Vol. 8, No. 1 35–44

ARTICLE

A Lys644Glu substitution in fibroblast growth factor receptor 3 (FGFR3) causes dwarfism in mice by activation of STATs and ink4 cell cycle inhibitors

Cuiling Li+, Lin Chen+, Tomoko Iwata[1], Motoo Kitagawa[2], Xin-Yuan Fu[2] and Chu-Xia Deng*

Genetics of Development and Diseases Branch, 10/9N105, National Institute of Diabetes, Digestive and Kidney Diseases and [1]Medical Genetics Branch, National Human Genome Research Institute, National Institutes of Health, 10 Center Drive, Bethesda, MD 20892, USA and [2]Department of Pathology, Yale University School of Medicine, New Haven, CT 06520, USA

Received September 30, 1998; Revised and Accepted October 26, 1998

Missense mutations of human fibroblast growth factor receptor 3 (FGFR3) result in several skeletal dysplasias, including hypochondroplasia, achondroplasia and thanatophoric dysplasia. To study the function of FGFR3 in bone growth and to create animal models for the FGFR3-related inherited skeletal disorders, we introduced a point mutation (Lys644Glu) into the murine FGFR3 genome using a knock-in approach. We found that the Lys644Glu mutation resulted in retarded endochondral bone growth with severity directly linked to the expression level of the mutated *Fgfr3*. Mice heterozygous for the mutation (*Fgfr3*$^{TD/+}$) expressed the mutant allele at ~20% of the wild-type level and exhibited a mild bone dysplasia. However, when the copy number of the mutant allele increased from one (*Fgfr3*$^{TD/+}$) to two (*Fgfr3*$^{TD/TD}$), the retardation of bone growth became more severe and showed phenotypes resembling those of achondroplasia patients, characterized by a dramatically reduced proliferation of growth plate cartilage, macrocephaly and shortening of the long bones, which was most pronounced in the femur. Molecular analysis revealed that expression of the mutant receptor caused the activation of Stat1, Stat5a and Stat5b, and the up-regulation of p16, p18 and p19 cell cycle inhibitors, leading to dramatic expansion of the resting zone of chondrocytes at the expense of the proliferating chondrocytes. The mutant growth plates consequently were in a less active state and generated fewer maturing and hypertrophic chondrocytes. These data provide direct genetic evidence that the point mutations in FGFR3 cause human skeletal dysplasias and uncover a mechanism through which the FGFR3 signals regulate bone growth by modulating expression of Stats and ink4 cell cycle inhibitors.

INTRODUCTION

Fibroblast growth factor receptor 3 (FGFR3) is a membrane-spanning tyrosine kinase that serves as a high affinity receptor for fibroblast growth factors (FGFs) (reviewed in ref. 1). It has been shown that mutations in the coding sequence of the *Fgfr3* gene result in several skeletal diseases in human, including achondroplasia (ACH), hypochondroplasia (HCH) and thanatophoric dysplasia (TD) (2–6). ACH, which is correlated with amino acid alterations in the transmembrane domain of FGFR3, is the most common form of dwarfism, with a frequency of ~1 in 15 000 live births. ACH patients exhibit a characteristic phenotype of rhizomelic dwarfism, relative macrocephaly, exaggerated lumbar lordosis and minimal proliferation of growth plate cartilage of long bones. Mutations in several different domains of FGFR3 cause TD, a common but more severe neonatal lethal skeletal dysplasia (5,7,8). Two major forms of TD have been reported (5). The TD type I (TD I) patients have relatively curved, short femurs, whereas the TD type II (TD II) patients have relatively straight femurs and severe cloverleaf skull (5). HCH is an autosomal dominant skeletal dysplasia with skeletal features that are similar to, but milder than, those observed in ACH and TD (6).

Targeted gene disruption has been used to study FGFR3 function. It was shown that loss of FGFR3 results in the overgrowth of long bones, a phenotype that is opposite to these human diseases (9,10). Thus, FGFR3 is essential for restraining chondrocyte proliferation—inhibiting, rather than promoting, bone growth and development. In light of this knockout

*To whom correspondence should be addressed. Tel: +1 301 402 7225; Fax: +1 301 496 0839; Email: chuxiad@bdg10.niddk.nih.gov
+These authors contributed equally to this work

phenotype, we suggested that the human diseases are caused by gain-of-function mutations that activate the negative growth control exerted by FGFR3 (9). Indeed, it has been demonstrated by several *in vitro* studies that mutations of FGFR3, which are responsible for ACH and TD, cause ligand-independent activation of the receptor (11–13).

To study further the function of FGFR3 in bone growth and to create mouse models for the FGFR3-related inherited skeletal disorders, we introduced the Lys644Glu (lysine 644 to glutamic acid) mutation, which corresponds to the Lys650Glu mutation found in human TD II patients (5), into the mouse genome using a knock-in approach. It was shown previously that FGFR3 carrying this mutation exhibits constitutive tyrosine kinase activity that activates STAT1 and up-regulates the cell cycle inhibitor $p21^{WAF1/CIP1}$ (14). Because $p21^{WAF1/CIP1}$ is known to be essential for the G_1/S checkpoint and can prevent cells from proliferating when overexpressed (15–19), it was proposed that the activation of $p21^{WAF1/CIP1}$ may be responsible for the inhibition of chondrocyte proliferation (14). We show here that introduction of the Lys644Glu mutation into the murine germline results in retarded endochondral bone growth whose severity is correlated directly to the expression level of the mutant allele. Molecular analysis revealed increased expression and activation of several Stat proteins, and up-regulation of ink4 family cell cycle inhibitors in the mutant mice that may be responsible for retarded endochondral bone growth and development.

RESULTS

Introduction of Lys644Glu mutation into murine FGFR3

Knock-in constructs *pFgfr3-TD* (Fig. 1A) and *pFgfr3-WT* carry a portion of *Fgfr3* cDNA from the *Eco*RI site in exon 5–exon 19, which encodes the 3′-untranslated region (20). These are followed by an SV40 poly(A) and a *pLoxpneo* cassette (21). The *pFgfr3-TD* contained a point mutation which causes the Lys644Glu conversion in the FGFR3. The *pFgfr3-WT* carried no mutation and was used as a knock-in control. The *Eco*RI site in exon 5 was used previously to create a loss-of-function allele by a *neo* gene insertion (9). Thus, the homologous recombination between these targeting vectors and the targeted locus is predicted to knock-in the cDNAs and concomitantly disrupt the endogenous gene. Both targeting vectors gave roughly the same targeting efficiency of ~5% of G418-resistant embryonic stem (ES) clones analyzed for homologous recombination. The presence of the introduced mutation in the targeted clones was confirmed by sequencing (data not shown).

Germline transmission was obtained from ES cells generated by the targeting of either the *pFgfr3-WT* or the *pFgfr3-TD* construct. Southern blot analysis or PCR for the presence of the neo^r gene indicated that ~50% of agouti offspring carried the introduced mutations. Mice heterozygous for the Lys644Glu mutation ($Fgfr3^{TD/+}$) were crossed with EIIa-Cre mice (22) to excise the *ploxpneo* gene from the germline (Fig. 1B). Mice both with and without the neo^r gene were analyzed and showed identical phenotypes. All the data provided below were obtained from the mice without the *neo* gene.

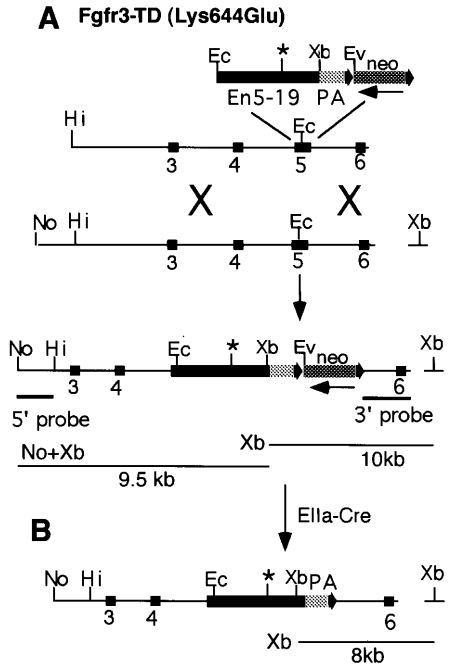

Figure 1. Knock-in of the Lys644Glu mutation into the *Fgfr3* locus. (**A**) Targeting vectors *pFgfr3-TD* and *pFgfr3-WT* (data not shown) carry a portion of *Fgfr3* cDNA from the *Eco*RI site in exons 5–19 (En5–19) followed by an SV40 poly(A) (PA) and a *pLoxpneo* cassette (21). The *pFgfr3-TD* contains the Lys644Glu mutation (*), while the *pFgfr3-WT* carries only the wild-type sequence. Targeting was detected using the 5′-flanking probe, which hybridizes to a band of 9.5 kb in the targeted allele upon *Not*I + *Xba*I digestion. The correct targeting event is confirmed using the 3′ internal probe, which detects a 10 kb fragment upon *Xba*I digestion. Ec, *Eco*RI; Ev, *Eco*RV; Hi, *Hin*dIII; No, *Not*I; Xb, *Xba*I. (**B**) Removal of the *pLoxpneo* gene by breeding with EIIa-Cre transgenic mice. The Cre-mediated deletion of the *neo* gene which is ~2 kb will generate an 8 kb fragment upon *Xba*I digestion followed by probing with the 3′ probe. The 5′ probe is a 2 kb *Not*I–*Hin*dIII fragment, and the 3′ probe is a 1.6 kb fragment that runs from the *Eco*RI site to the end of the targeting construct.

FGFR3 Lys644Glu mutation results in dwarf mice

Mice heterozygous for the Lys644Glu mutation ($Fgfr3^{TD/+}$) were smaller, and displayed a significantly shorter tail length than their wild-type littermates (Fig. 2A). F_2 offspring were generated by intercrossing F_1 $Fgfr3^{TD/+}$ mice. At birth, mice homozygous for the mutation ($Fgfr3^{TD/TD}$) were normal. However, they exhibited pronounced dwarfism during postnatal development as judged by dramatically reduced tail length and body weight (Fig. 2). Tail lengths of the $Fgfr3^{TD/TD}$, $Fgfr3^{TD/+}$ and their wild-type controls were about the same at birth. However, the tails of $Fgfr3^{TD/TD}$ mice grew more slowly and stayed at ~70% of those of the controls (we used wild-type mice for all controls) at most time points measured (Fig. 2B). The $Fgfr3^{TD/+}$ mice exhibited intermediate lengths between the wild-type control and the $Fgfr3^{TD/TD}$ (Fig. 2A and B). Since the FGFR3-deficient mice have longer tails than wild-type (Fig. 2A and ref. 9), the short tails of $Fgfr3^{TD/TD}$ mice suggest that the Lys644Glu mutation in FGFR3 retards the vertebral bone growth and results in a phenotype opposite to that caused by the loss-of-function mutation of FGFR3. The body weight of the $Fgfr3^{TD/TD}$ mice was ~70% of the control weight, whereas that of the $Fgfr3^{TD/+}$ mice

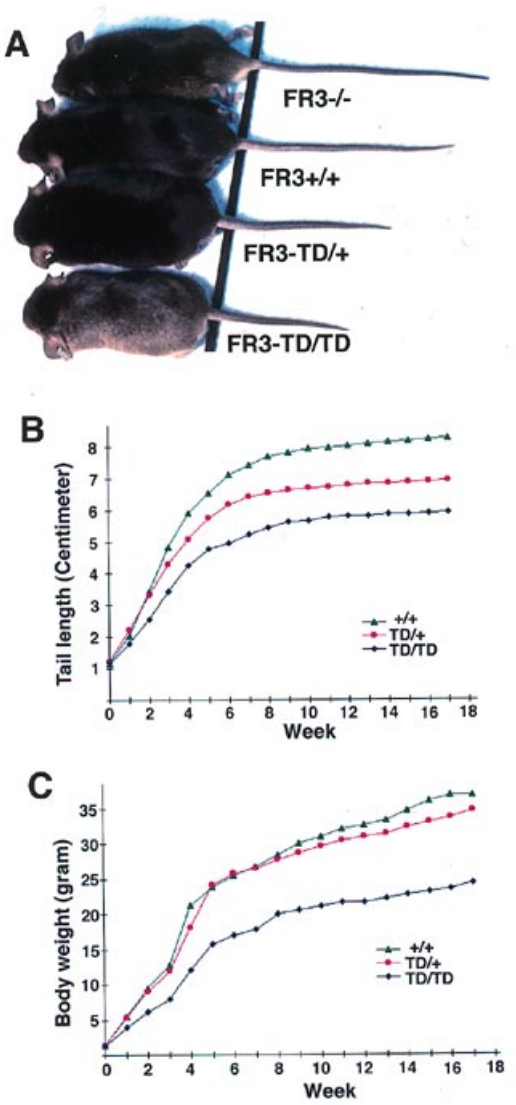

Figure 2. The Lys644Glu mutation results in dwarfism. (**A**) A comparison of tail lengths of 2-month-old mice. Genotypes are as indicated. (**B** and **C**) Quantitative measurements of tail length (B) and body weight (C) of wild-type, *Fgfr3*$^{TD/+}$ and *Fgfr3*$^{TD/TD}$ mice. Each point represents data from an average of six male mice. Standard deviation is <5%. The FGFR3-deficient (FR3$^{-/-}$) mouse was created previously (9). Body weights and tail lengths of the knock-in control *Fgfr3*$^{WT/WT}$ mice were virtually identical to those of wild-type mice when measured at 1–4 and 14–18 weeks (data not shown).

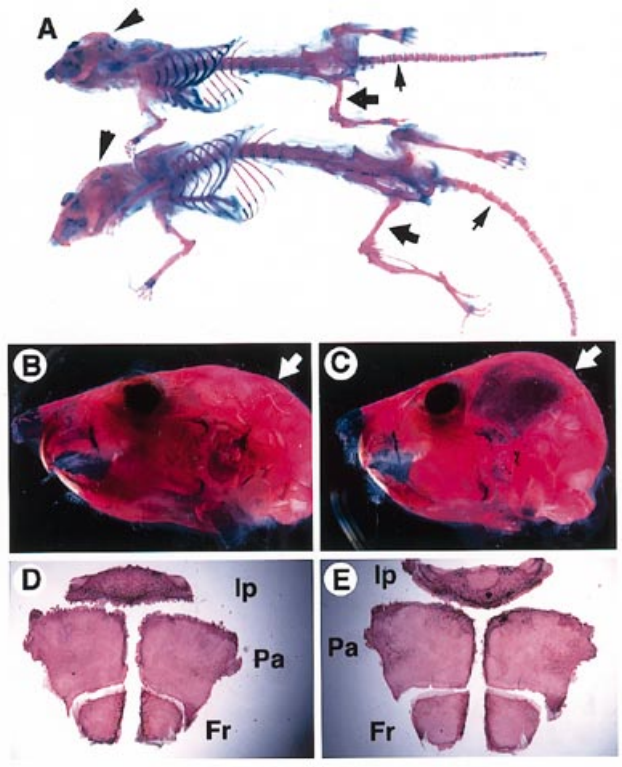

Figure 3. Analysis of skeleton and skull of *Fgfr3*$^{TD/TD}$ mice. (**A**) Skeletons of 2-month-old *Fgfr3*$^{TD/TD}$ (upper) and control mice. The femurs (large arrows) and vertebrate bones (small arrows) of mutant mice are much shorter than those of controls. (**B** and **C**) Head of control (B) and mutant (C) mice showing macrocephaly in mutant mice (C). (**D** and **E**) Flat bones of control (D) and mutant (E). No difference was found in bones formed by intramembranous ossification between the mutants and controls. Ip, interparietal bone; Pa, parietal bone; Fr, frontal bone.

was ~90% of the control weight, between 21 and 126 days post-partum (p21–126) (Fig. 2C).

Whole skeletons from *Fgfr3*$^{TD/TD}$, *Fgfr3*$^{TD/+}$ and wild-type littermates were examined by Alizarin staining. The *Fgfr3*$^{TD/TD}$ mice exhibited shortening in the length of all bones formed by endochondral ossification (Fig. 3A). When measured at p20 and p90 (n = 6 in all measurements), the wild-type humeri were of mean lengths (±SD) 0.92 ± 0.2 and 1.30 ± 0.02 cm, respectively, whereas those of the homozygous littermates were 0.70 ± 0.01 (76% of the wild-type) and 0.91 ± 0.01 (70%), respectively. During the same period, the lengths of the control femurs were an average of 1.07 ± 0.03 and 1.66 ± 0.05 cm, respectively, while the *Fgfr3*$^{TD/TD}$ femurs were 0.73 ± 0.03 (68%) and 1.08 ± 0.02 (65%), respectively. The tails were reduced to 70% in length, suggesting severe shortening of the tail vertebrae. However, the spinal columns are least affected, with average lengths of 83% of the wild-type lengths. There was a decrease in the interpedicular distances between vertebral bodies that was proportional to the reduction in the lengths of vertebral bodies. These data indicate that, among all other types of bones measured, the Lys644Glu mutation has its strongest effect in femurs.

Macrocephaly was observed in the *Fgfr3*$^{TD/TD}$ mice (Fig. 3C and D). An examination of bones formed by intramembranous ossification (flat bones) revealed no difference in sizes and gross morphology between mutant mice and their wild-type littermates (Fig. 3D and E). This suggests that the macrocephaly may be caused by imbalanced growth between bones formed by the two different pathways, i.e. normal growth of bones formed by intramembranous ossification and slower growth of bones formed by endochondral ossification in the skull.

As a control for the knock-in strategy, mice heterozygous and homozygous for the FGFR3-WT construct were also examined at 1–4, 14 and 18 weeks. They were found to be phenotypically

normal (data not shown), suggesting that the skeletal dysplasia is related specifically to the introduced Lys644Glu mutation.

The FGFR3 Lys644Glu mutation inhibits proliferation of growth plate chondrocytes

Growth plates of the mutant mice were examined. Chondrocytes in wild-type growth plates can be divided into four different cell types, i.e. resting, proliferating, maturing and hypertrophic chondrocytes (Fig. 4A). In mutant growth plates, these cells were less distinct by histological standards. Mutant proliferation and maturation zones were very disorganized and failed to form long chondrocyte columns, which are usually found in wild-type growth plates (Fig. 4A and B). The height of the mutant hypertrophic zone was reduced compared with that of the control (Fig. 4A and B). *In situ* hybridization using a cell lineage marker for maturing chondrocytes (*Indian hedgehog*, *Ihh*) revealed weaker staining (Fig. 4C and D), suggesting a reduction in the number of *Ihh*-expressing cells in the mutant plates. Collagen type II is normally expressed in resting and hypertrophic chondrocytes at a low level and at much higher levels in the proliferating and maturing zones (Fig. 4E). Staining for this marker revealed smaller proliferating and maturing zones in the mutant growth plates (Fig. 4F). This observation suggests that the mutant chondrocytes were in a less proliferative and maturing state. Moreover, in the wild-type growth plates, the resting chondrocytes were present in a relatively narrow zone (bar in Fig. 4E). In contrast, this zone was dramatically expanded in mutant plates (bar in Fig. 4F). All mutant growth plates examined ($n > 10$) were wider than controls mainly because of the expansion of the resting zone. Hypertrophic chondrocytes are terminal differentiation products of the proliferating and maturing chondrocytes. The reduced activity of the proliferating chondrocytes in mutant mice generated fewer hypertrophic chondrocytes as revealed by the expression domain of collagen type X which marks the hypertrophic zone (Fig. 4G and H).

Proliferation of mutant chondrocytes was assessed further by [^{3}H]thymidine incorporation. The radioactively labeled chondrocytes in the normal growth plate were present as a zone adjacent to the resting chondrocytes (Fig. 4I), suggesting that this area had undergone DNA replication. In contrast, the [^{3}H]thymidine-labeled cells in mutant growth plates were not only scattered, but also much fewer in number (Fig. 4J). The intensity of signals in each mutant cell was ~70% of that of control cells (Fig. 4I and J). This experiment indicates that the mutant plates have much lower activities in chondrocyte cell proliferation, which results in pronounced dwarfism.

The FGFR3 Lys644Glu mutation activates Stat1, Stat5a and Stat5b

It has been shown previously that the FGFR3 Lys644Glu activates Stat1 (14). To determine if this is the case in the *Fgfr3*$^{TD/TD}$ mice, we examined Stat1 expression in mutant epiphyseal growth plates by immunohistochemistry. In normal growth plates, Stat1 is expressed at low levels (Fig. 5). In mutant growth plates, the expression of Stat1 is significantly increased (Fig. 5). Because Stats exist as a gene family, we also checked the expression of two other Stats, i.e. Stat5a and Stat5b, in growth plates. In wild-type mice, these proteins were expressed at a very low level in the proliferation zone and at a higher level in resting and maturing zones (Fig. 5B and C). Mutant mice exhibited a

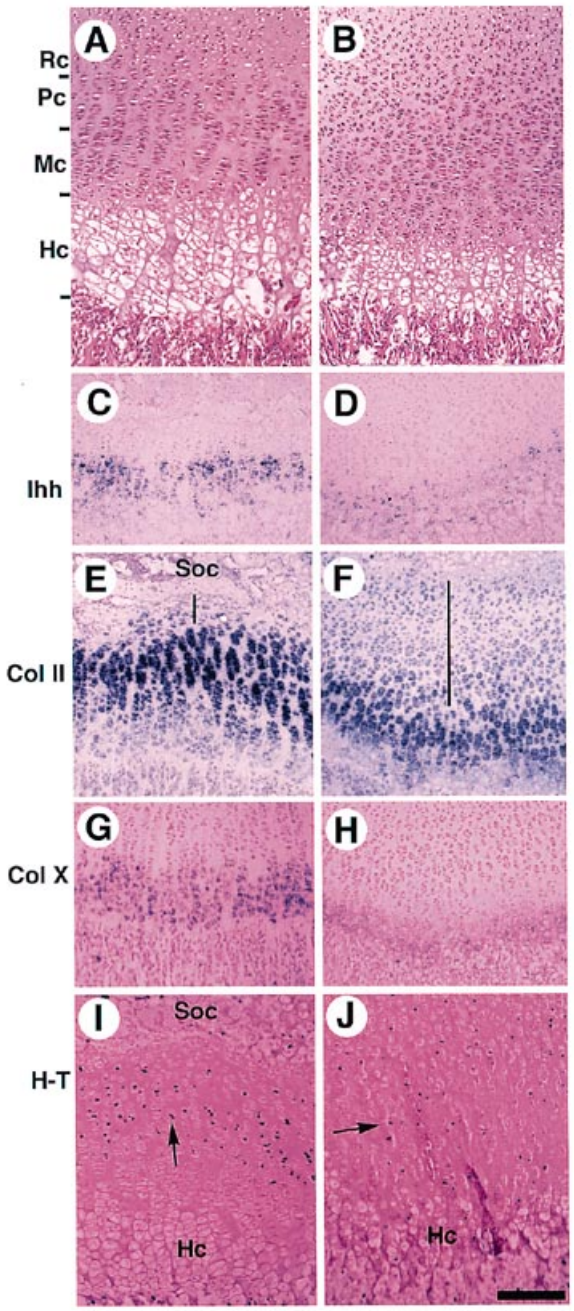

Figure 4. Histology and *in situ* hybridization. Wild-type (A, C, E, G and I) and mutant (B, D, F, H and J) growth plates from ~3-week-old femurs. Whole epiphyseal plates are shown in (A, B, E and F), whereas all other panels show only partial plates. (**A** and **B**) Histological sections. Chondrocytes in the wild-type growth plates are divided into four distinct zones, i.e. resting (Rc), proliferating (Pc), maturing (Mc) and hypertrophic (Hc) chondrocytes. In the mutant plates (B), the demarcation of each zone is not clear. (C–J) *In situ* hybridization using *Ihh* for Mc (**C** and **D**), collagen type II for Pc (**E** and **F**) and collagen type X for Hc (**G** and **H**). Bars mark the resting zone of wild-type (E) and mutant (F) chondrocytes, respectively. (**I** and **J**) [^{3}H]thymidine incorporation. The labeled cells in wild-type mark the Pc zone. In mutant plates, the labeled cells are fewer in number and scattered, suggesting that the majority of the cells are in a quiescent state. Soc: secondary ossification center. Bar, 185 μm (A and B), 230 μm (C–H) and 180 μm (I and J).

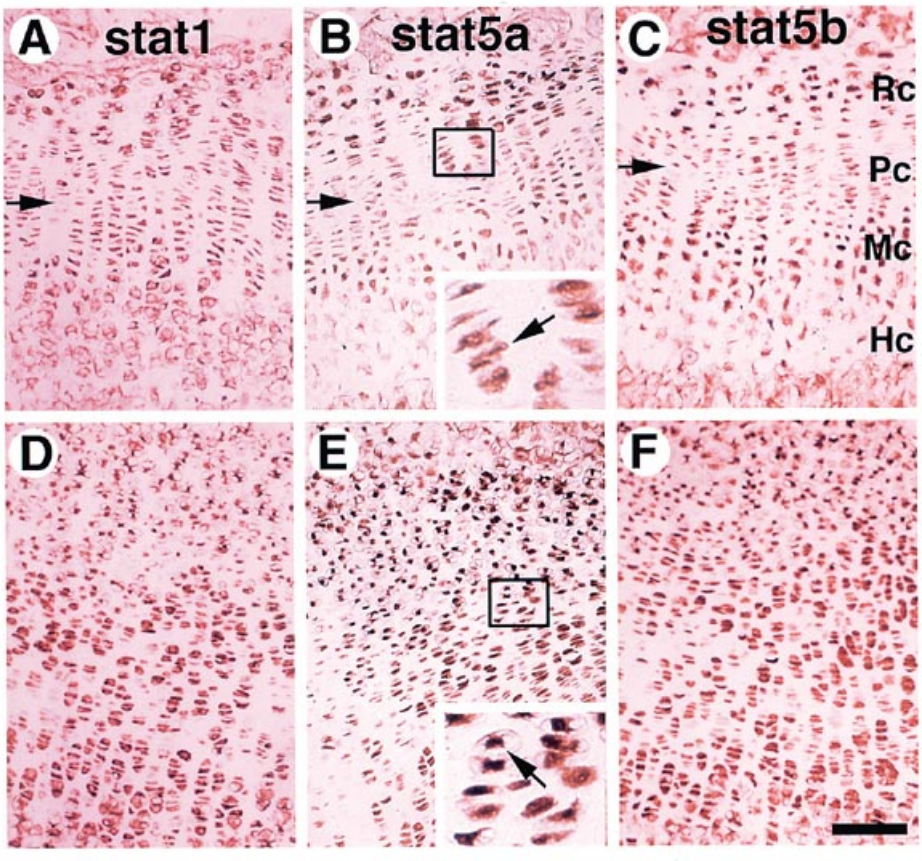

Figure 5. Immunohistochemistry of Stat proteins. (**A** and **D**), (**B** and **E**) and (**C** and **F**) are stained with antibodies to Stat1, Stat5a and Stat5b, respectively. In wild-type growth plates (A–C), the staining was the weakest in the proliferating (Pc) zone, and most cells showed cytoplasmic localization (enlarged box in B). In the mutant plates (D–F), the staining is much stronger, and many cells show nuclear staining (enlarged box in E). Bars, 100 μm in all panels.

much stronger staining of these proteins, especially Stat5a, in virtually all chondrocytes except for the hypertrophic chondrocytes (Fig. 5E and F). Translocation of Stat proteins into the nucleus was used as an indicator of Stat activation, because the unphosphorylated Stat proteins were in the cytoplasm, and the activated forms were translocated into nuclei (23,24). Close examination revealed nuclear localization of Stat proteins in many mutant cells (Fig. 5E), suggesting that these proteins were activated.

Lys644Glu mutation activates cell cycle inhibitors p16, p18 and p19, but not p21$^{WAF1/CIP1}$

It has been suggested that Stat activation and p21$^{WAF1/CIP1}$ induction might together be responsible for the TD II FGFR3-induced bone defects (14). To test this in our mouse model, we examined expression of p21$^{WAF1/CIP1}$ in growth plate chondrocytes by immunohistochemistry using an antibody to the p21$^{WAF1/CIP1}$ protein. Analysis of four 2–3-week-old mutant mice revealed either no or only a slight increase in p21$^{WAF1/CIP1}$ expression in the mutant growth plates versus controls (Fig. 6A and B). Because the observed increase was so modest, we were uncertain whether or not p21$^{WAF1/CIP1}$ was involved in FGFR3-dependent bone deformation *in vivo*. We therefore decided to examine this further by introducing the Lys644Glu mutation into a p21-null background generated earlier (18). Comparison between p21-null/ *Fgfr3*$^{TD/TD}$ and *Fgfr3*$^{TD/TD}$ mice revealed no difference in the lengths of the endochondral bones or in the morphology of growth plate chondrocytes (data not shown), indicating that the loss of p21$^{WAF1/CIP1}$ in *Fgfr3*$^{TD/TD}$ mice did not rescue the skeletal dysplasia. Thus, contradictory to the previous finding, our observations suggest that p21$^{WAF1/CIP1}$ does not play a major role in the growth retardation caused by the FGFR3 Lys644Glu mutation.

Because our earlier data indicated that the mutant growth plate chondrocytes were generally in a much lower proliferative state, we examined expression of several additional cell cycle inhibitors, including p16, p18 and p19, which belong to the ink4 family. Our data revealed a significant increase in the expression of these proteins in mutant growth plates (Fig. 6C–F for p18 and p19; p16 not shown). The observed increase may be caused by the introduction of the Lys644Glu mutation, since mice carrying the wild-type knock-in cDNA showed no increase in these proteins (Fig. 6G). Consistently, the growth plates of *Fgfr3*$^{WT/WT}$ mice were apparently normal compared with wild-type plates (Fig. 6H and I). These data revealed the involvement of the ink4 cell cycle inhibitors in mediating the effect of FGFR3 Lys644Glu mutation on bone growth .

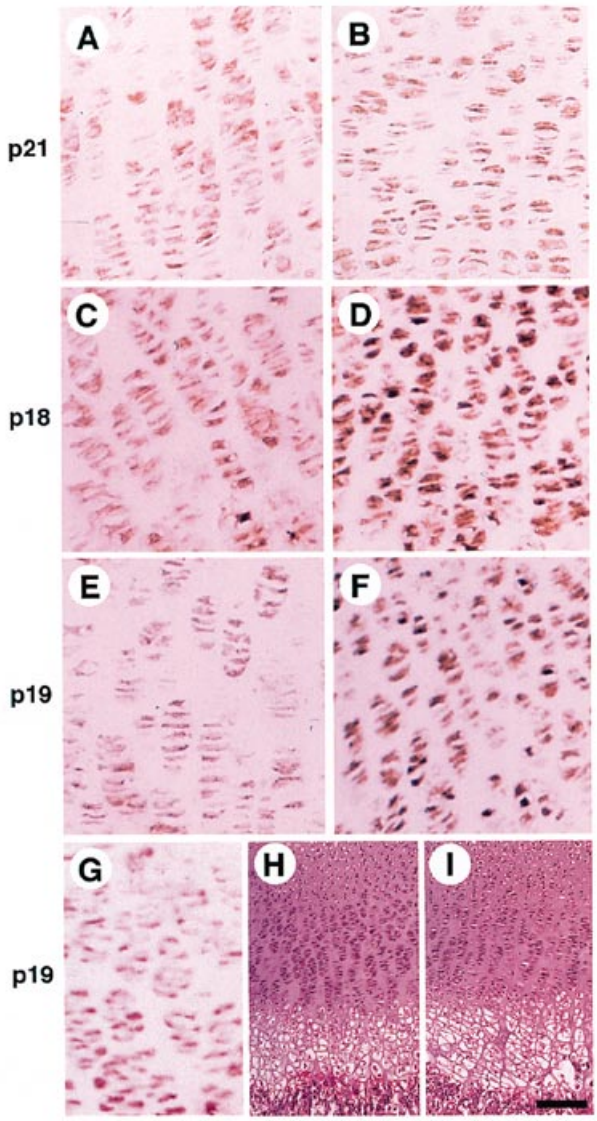

Figure 6. Immunohistochemistry of cell cycle inhibitors. Antibodies to p21, p18 and p19 as indicated. (**A**, **C** and **E**) Wild-type growth plates and (**B**, **D** and **F**) mutant plates. (**G** and **H**) Growth plates of knock-in controls (*Fgfr3*$^{WT/WT}$). A much stronger signal is found in the mutant cells stained with p18 and p19 (D and F). In contrast, no obvious increase in staining was found in the p21 stained mutant cells (B), or p19 stained knock-in (*Fgfr3*$^{WT/WT}$) controls (G). (**H** and **I**) H&E images of the *Fgfr3*$^{WT/WT}$ (H) and wild-type (I) growth plate showing normal structures. Bars, 100 μm (A–G) and 400 μm (H and I).

Expression of FGFR3 in *Fgfr3*$^{TD/TD}$ mice

The Lys650Glu mutation in human results in TD II, which causes postnatal lethality. TD II patients also develop severe cloverleaf skulls. However, our analysis indicated that the *Fgfr3*$^{TD/TD}$ mice did not have these features, rather they displayed phenotypes resembling those of achondroplasia. While this discrepancy could be due simply to a difference in species, we decided to check the expression levels of the knock-in alleles in the mutant mice. RNAs from brains of wild-type (+/+), Fgfr3-TD and Fgfr3-WT (knock-in control) mice were examined by northern blot. Neither *Fgfr3*$^{WT/WT}$ control nor *Fgfr3*$^{TD/TD}$ mice exhibited the wild-type allele (3.5 kb). However, both expressed the knock-in alleles at ~20% of the wild-type level (Fig. 7A). This observation indicated that the knock-in alleles, irrespective of the point mutation, were transcribed or spliced less efficiently. *In situ* hybridization on the growth plates of wild-type and mutant mice confirmed the observation that the mutant allele is expressed at a much lower level (Fig. 7B–E). We next stained the growth plates with an antibody to FGFR3. *Fgfr3*$^{WT/WT}$ growth plates (Fig. 7H) were found to express FGFR3 protein at a level much lower than that of the controls (Fig. 7F). In contrast, the *Fgfr3*$^{TD/TD}$ growth plates showed an intensity comparable with that of the controls (Fig. 7I). It was reported that TD I patients displayed much higher levels of FGFR3 protein in growth plate chondrocytes with no increase in the level of the corresponding mRNA (25). Our finding is consistent with this observation, because transcripts of the Lys644Glu allele at ~20% of the wild-type level generated an amount of protein which is comparable with the wild-type level. Taken together, these findings suggest that either the FGFR3-TD allele is translated more efficiently or the mutant protein is more stable, or a combination of the two.

DISCUSSION

FGFRs exist as a gene family of four members that mediate signals of at least 17 ligands (reviewed in ref. 1). Mutations in coding regions of three receptors (FGFR1–3) are found in at least nine skeletal dysplasias in human (26–30). Significantly, all of these disorders are dominant, with craniofacial, appendicular and/or axial bone abnormalities resulting from missense mutations in the FGFRs. Studies carried out *in vitro* showed that these mutations result in activation of the tyrosine kinase of the receptors, suggesting that these diseases are caused by gain-of-function rather than loss-of-function mechanisms (11,12). Consistent with these findings, we and others have shown previously that mice heterozygous or homozygous for loss-of-function mutations of FGFR1, FGFR2 or FGFR3 do not exhibit any phenotypes that resemble the human disorders (9,10,31–35). Interestingly, FGFR3-deficient mice exhibited defects characterized by overgrowth of bones formed by endochondral ossification, leading to a conclusion that FGFR3 is a negative regulator of bone growth (9). In the present study, we show that mice carrying the Lys644Glu mutation exhibit pronounced dwarfism and macrocephaly. These phenotypes are similar to those observed in the FGFR3-related human diseases but opposite to phenotypes of the FGFR3$^{-/-}$ mice (9,10). Because control mice carrying the wild-type knock-in allele (*Fgfr3*$^{WT/WT}$) are normal, we conclude that it is the Lys644Glu mutation that is responsible for the observed bone defects. Thus, our study provides direct genetic evidence that the point mutations in FGFR3 cause human skeletal dysplasias. The dwarf mouse we created may potentially be useful as an animal model for further studies on these skeletal diseases.

Skeletal dysplasias caused by FGFR3 display varying degrees of severity. The transmembrane mutations that result in ACH seem to be weaker alleles than those that generate the TD phenotype, which usually results in postnatal lethality. The weakest allele is HCH, which is difficult to recognize in early childhood for some patients (36). Several lines of evidence have indicated that the varying severity of these diseases is a quantitative phenomenon. It was observed that patients who are

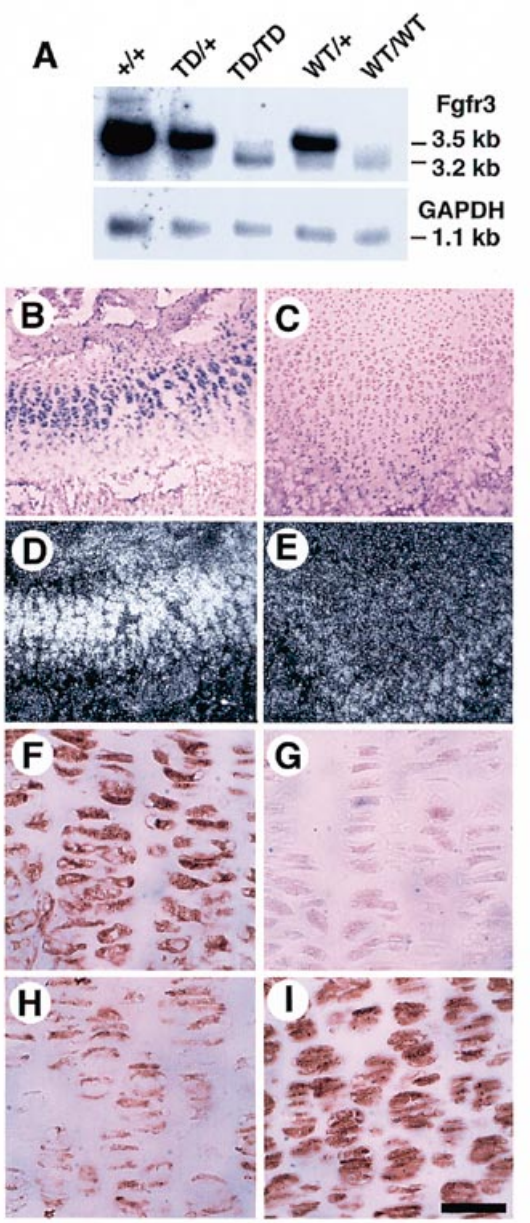

Figure 7. Expression of knock-in alleles. (**A**) Northern blot analysis of RNAs isolated from brains of 2-month-old mice. Genotypes were as indicated. The endogenous transcripts are ~3.5 kb and the knock-in alleles are 3.2 kb, when hybridized with a probe [nucleotides 226–788 of the FGFR-3 cDNA (20)] that can detect both alleles. The same filter is hybridized using a probe for GAPDH to provide a loading control. (**B**–**E**) *In situ* hybridization of wild-type (B, bright view; D, dark view) and $Fgfr3^{TD/TD}$ (C, bright view; E, dark view) growth plates from ~3-week-old mice using the same FGFR3 cDNA probe. The staining in the control is in the proliferating and maturing chondrocytes (B and D). The mutant exhibited a much weaker intensity (C and E). (**F**–**I**) Immunohistochemical staining of FGFR3 protein with an antibody to FGFR3 in wild-type (F), $Fgfr3^{WT/WT}$ (H) and $Fgfr3^{TD/TD}$ (I) mice. (G) shows an antibody-minus control. Bar, 200 µm (B–E) and 35 µm (F–I).

homozygous for the ACH alleles exhibit phenotypes similar to that of the TD patients (37). Moreover, patients heterozygous for both ACH and HCH alleles have a stronger phenotype than that seen with each allele alone (38). Consistently, *in vitro* analyses indicate that FGFR3 cDNAs carrying mutations for ACH and TD exhibited a graded activation of their tyrosine kinase activities, with wild-type < ACH < TD (11). These observations could be accommodated by assuming that the quantitative difference in phenotype is due to alleles with varying degrees of ligand-independent activation generated by missense mutations occurring at different domains within the receptor. In our mice, the transcripts of knock-in alleles were expressed at a much lower level than that of the wild-type allele. Thus, the FGFR3-TD allele, which correlates with the most severe phenotype in human, results in a milder bone dysplasia when it is expressed at a lower level. However, when the copy number increases from one ($Fgfr3^{TD/+}$) to two ($Fgfr3^{TD/TD}$), the retardation of bone growth becomes more severe. This observation, from a different angle, demonstrates that the varying severity associated with the FGFR3-related skeletal dysplasias could be contributed by the quantity of mutant proteins.

We have not determined the mechanism underlying the reduced expression of the *Fgfr3* knock-in alleles. It is unlikely to be caused by the Lys644Glu mutation since the knock-in control, which carries no mutation, exhibits a similar reduction. Rather, it may suggest that the *Fgfr3* locus is sensitive to such a manipulation. The knock-in strategy causes the deletion of several introns, which may contain regulatory sequences required for maintaining normal expression. Alternatively, the knock-in construct has its own SV40 poly(A). If this poly(A) is weaker than the endogenous one, it may also cause the observed reduction.

FGFRs usually exist in an inactivated monomer form, and become activated upon binding to their ligands. The activated receptors interact with the SH (Src homology) domain-containing adaptor molecules, such as Grb2, and eventually activate MAP kinase (39). However, we found that FGFR3 carrying the Lys644Glu mutation could not activate MAP kinase (X.-Y. Fu, unpublished data). Instead, it activated STAT1, resulting in the up-regulation of the cell cycle inhibitor $p21^{WAF1/CIP1}$. It was therefore proposed that the activation of $p21^{WAF1/CIP1}$ may be responsible for the inhibition of chondrocyte proliferation (14). Now using the dwarf mice created by the present study, we re-examined some of our previous work. While the new data confirmed the activation of Stat1 by the FGFR3-TD mutation, they also revealed the activation of two other members of this family, Stat5a and Stat5b, suggesting a broader effect of FGFR3 activation on the Stats. However, an interesting finding, which is contradictory to the previous study, is that the retarded bone growth in $Fgfr3^{TD/TD}$ mice is unlikely to be mediated by $p21^{WAF1/CIP1}$. We found no evidence of increased p21 expression in mutant growth plates compared with wild-type plates. Consistently, introduction of a p21-null background into the $Fgfr3^{TD/TD}$ mice did not have any apparent influence on the phenotype. Surprisingly, we found that the activation of FGFR3 up-regulated a number of cell cycle inhibitors that belong to the ink4 family, including p16, p18 and p19. This, in turn, results in cell cycle arrest and expansion of resting zone chondrocytes at the expense of proliferating and maturing chondrocytes. Together with the fact that the loss of p21 cannot rescue dwarfism of $Fgfr3^{TD/TD}$ mice, these observations suggest that the activated Stats signals in mice may function through members of the ink4 family instead of through p21. This issue is subject to further investigation because it is contradictory to an observation that activation of Stat1 in chondrocytes from human TD II fetuses results in increased p21 expression (14).

Chondrogenesis is a process that involves both proliferation and differentiation of chondrocytes. Multiple growth factors and signaling molecules, including thyroid hormones, Indian hedgehog (Ihh) and FGFs/FGFRs, have been implicated in this process (9,40–44). It was demonstrated recently that PTHrP and Ihh constitute a paracrine feedback loop that plays a major role in regulating chondrocyte differentiation (45). In contrast, FGFs and their receptors have been implicated in chondrocyte proliferation and/or differentiation (9,46). In the present study, we show that *Fgfr3* transcripts are in both proliferating and maturing chondrocytes (Fig. 7B and D). Introduction of the TD II-FGFR3 causes both poor proliferation and reduced terminal differentiation of mutant growth plate chondrocytes, based on the paucity of [^{3}H]thymidine-labeled cells and the reduced intensities of *Ihh* and collagen type X staining. However, for the following reasons, we believe that the TD II-FGFR3 may have a stronger effect on the proliferation rather than the differentiation. First, we showed previously that loss of FGFR3 caused an increased proliferation of proliferating chondrocytes, leading to faster bone growth (9). Second, we found in an *in vitro* system that expression of the TD II-FGFR3, but not the WT-FGFR3, inhibited proliferation of the transfected cells (14). We now show the same effect of the TD II-FGFR3 on the proliferating chondrocytes in mutant growth plates as demonstrated by the reduced number of [^{3}H]thymidine-positive cells (Fig. 4I and J). The expression of the mutant FGFR3 in the proliferating chondrocyte must have repressed the proliferative activity of the proliferating chondrocytes and kept them in a relatively quiescent state, leading to the expansion of the resting zone chondrocytes (Fig. 4E and F). The reduction of the proliferating zone consequently results in the reduced terminal differentiation of the mutant chondrocytes.

In summary, we showed that a mutation which activates FGFR3 causes dwarfism in mice. Our data support the hypothesis that FGFR3 functions as a negative regulator for endochondral bone growth, as proposed previously (9). The FGFR3 signals normally are regulated in a ligand-dependent fashion so that balanced long bone growth can be achieved. However, this balance can be broken by either loss-of-function mutations of FGFR3, which result in accelerated bone growth, or gain-of-function mutations of FGFR3, which primarily inhibit chondrocyte proliferation. The action of mutant FGFR3 in bone growth is most likely mediated through Stat proteins. The activated STATs, in turn, directly or indirectly up-regulate cell cycle inhibitors, limiting the proliferation of the chondrocytes, abnormally impeding bone growth and causing dwarfism.

MATERIALS AND METHODS

Targeting vectors

The FGFR3 expression vector pMo/mFR3/SV (20), which carries a point mutation of Lys644Glu (14), was digested by *Eco*RI at nucleotides 788–793 and by *Sac*II at the 3′ end of the expression unit to generate an *Eco*RI–*Sac*II fragment. After attaching a *ploxpneo* gene (21) to the *Sac*II site, this fragment was then inserted into an 8 kb *Hin*dIII–*Sal*I genomic fragment of the *Fgfr3* gene through an *Eco*RI site to generate the targeting vector, *pFgfr3-TD* (Fig. 1A). The *Eco*RI site previously was believed to be in exon 3 of the *Fgfr3* gene (9). It should be, however, in exon 5 based on a thorough study of the *Fgfr3* genomic structure (47). A control vector, *pFgfr3-WT*, which contains no mutation, was generated similarly.

Homologous recombination in ES cells and generation of germline chimeras

TC1 ES cells (9) were transfected with *Not*I-digested *pFgfr3-WT* and *pFgfr3-TD*, respectively. The culture, electroporation and selection of TC1 cells were carried out as described (33). ES cell colonies that were resistant to G418 were analyzed by Southern blot analysis for homologous recombination events within the *Fgfr3* locus. Genomic DNAs from these clones and the parental TC1 cell line were digested with *Not*I + *Xba*I or *Xba*I alone, and then probed with the 5′-flanking or 3′-internal fragments specific to the *Fgfr3* sequence (Fig. 1A).

ES cells heterozygous for the targeted mutation were microinjected into C57BL/6 blastocysts to obtain germline transmission. Male chimeras (identified by the presence of agouti coat color) were mated with NIH Black Swiss females (Taconic). Germline transmission was confirmed by agouti coat color in the F_1 animals, and all agouti offspring were tested for the presence of the mutant *Fgfr3* allele by Southern analysis or PCR.

Genotype analysis

Genotypes were determined by Southern blotting or PCR. For PCR analysis, the wild-type *Fgfr3* allele was detected by using a 5′ oligonucleotide (5′-GGCTCCTTATTGGACTCGC-3′), which is located in intron 4, and a 3′ oligonucleotide (5′-TCACTGC-CTAGAATGGCTGTC-3′), which is located in exon 7. This primer pair flanks the *Eco*RI site and amplifies an ~500 bp fragment from the wild-type *Fgfr3* gene. It only amplifies an ~350 bp fragment from the knock-in allele because of the deletion of introns 5 and 6.

Skeleton staining

Animals were euthanized by asphyxiation in CO_2. After removing their skins, the carcasses were eviscerated, fixed in 95% ethanol, stained with Alizarin Red S and Alcian Blue, cleared by KOH treatment, and stored in glycerol as described (48).

Histology and antibody staining

Histological sections and immunohistochemistry were performed using standard procedures. Antibodies to p18 and p19 were provided by Y. Xiong (49). The antibody for FGFR3 is from D. Ornitz (11). The antibody to p21 was purchased from Santa Cruz Biotechnology.

Northern blots and *in situ* hybridization

Northern blots and *in situ* hybridization were performed using standard procedures. The *Fgfr3* probe is a 562 bp *Nco*I–*Eco*RI fragment from nucleotides 226–788 of the FGFR-3 cDNA (20). The collagen type II and type X were obtained from B. Olsen. *Ihh* was from A. McMahan. Slides were dipped in emulsion (Kodak NTB-2) and exposed for 4–15 days before developing.

ACKNOWLEDGEMENTS

We thank B. Olsen for collagen type II and type X, A. McMahan for *Ihh* probes, and H. Westphal for EIIa-Cre mice. We thank D. Ornitz for FGFR3 and Y. Xiong for p16, p18 and p19 antibodies.

We are grateful to members of the Deng lab for helpful discussions and critical reading of the manuscript.

REFERENCES

1. Martin, G.R. (1998) The roles of FGFs in the early development of vertebrate limbs. *Genes Dev.*, **12**, 1571–1586.
2. Thompson, L.M., Raffioni, S., Wasmuth, J.J. and Bradshaw, R.A. (1997) Chimeras of the native form or achondroplasia mutant (G375C) of human fibroblast growth factor receptor 3 induce ligand-dependent differentiation of PC12 cells. *Mol. Cell. Biol.*, **17**, 4169–4177.
3. Rousseau, F., Bonaventure, J., Legeai-Mallet, L., Pelet, A., Rozet, J.M., Maroteaux, P., Le Merrer, M. and Munnich, A. (1994) Mutations in the gene encoding fibroblast growth factor receptor-3 in achondroplasia. *Nature*, **371**, 252–254.
4. Shiang, R., Thompson, L.M., Zhu, Y.Z., Church, D.M., Fielder, T.J., Bocian, M., Winokur, S.T. and Wasmuth, J.J. (1994) Mutations in the transmembrane domain of FGFR3 cause the most common genetic form of dwarfism, achondroplasia. *Cell*, **78**, 335–342.
5. Tavormina, P.L., Shiang, R., Thompson, L.M., Zhu, Y.Z., Wilkin, D.J., Lachman, R.S., Wilcox, W.R., Rimoin, D.L., Cohn, D.H. and Wasmuth, J.J. (1995) Thanatophoric dysplasia (types I and II) caused by distinct mutations in fibroblast growth factor receptor 3. *Nature Genet.*, **9**, 321–328.
6. Bellus, G.A., McIntosh, I., Smith, E.A., Aylsworth, A.S., Kaitila, I., Horton, W.A., Greenhaw, G.A., Hecht, J.T. and Francomano, C.A. (1995) A recurrent mutation in the tyrosine kinase domain of fibroblast growth factor receptor 3 causes hypochondroplasia. *Nature Genet.*, **10**, 357–359.
7. Orioli, I.M., Castilla, E.E. and Barbosa-Neto, J.G. (1986) The birth prevalence rates for the skeletal dysplasias. *J. Med. Genet.*, **23**, 328–332.
8. Rousseau, F., Bonaventure, J., Le Merrer, M., Maroteaux, P. and Munnich, A. (1996) [Mutations of FGFR3 gene cause 3 types of nanisms with variable severity: achondroplasia, thanatophoric nanism and hypochondroplasia]. *Ann. Endocrinol. (Paris)*, **57**, 153.
9. Deng, C., Wynshaw-Boris, A., Zhou, F., Kuo, A. and Leder, P. (1996) Fibroblast growth factor receptor 3 is a negative regulator of bone growth. *Cell*, **84**, 911–921.
10. Colvin, J.S., Bohne, B.A., Harding, G.W., McEwen, D.G. and Ornitz, D.M. (1996) Skeletal overgrowth and deafness in mice lacking fibroblast growth factor receptor 3. *Nature Genet.*, **12**, 390–397.
11. Naski, M.C., Wang, Q., Xu, J. and Ornitz, D.M. (1996) Graded activation of fibroblast growth factor receptor 3 by mutations causing achondroplasia and thanatophoric dysplasia. *Nature Genet.*, **13**, 233–237.
12. Webster, M.K. and Donoghue, D.J. (1996) Constitutive activation of fibroblast growth factor receptor 3 by the transmembrane domain point mutation found in achondroplasia. *EMBO J.*, **15**, 520–527.
13. Webster, M.K., D'Avis, P.Y., Robertson, S.C. and Donoghue, D.J. (1996) Profound ligand-independent kinase activation of fibroblast growth factor receptor 3 by the activation loop mutation responsible for a lethal skeletal dysplasia, thanatophoric dysplasia type II. *Mol. Cell. Biol.*, **16**, 4081–4087.
14. Su, W.C., Kitagawa, M., Xue, N., Xie, B., Garofalo, S., Cho, J., Deng, C., Horton, W.A. and Fu, X.Y. (1997) Activation of Stat1 by mutant fibroblast growth-factor receptor in thanatophoric dysplasia type II dwarfism. *Nature*, **386**, 288–292.
15. Harper, J.W., Adami, G.R., Wei, N., Keyomarsi, K. and Elledge, S.J. (1993) The p21 Cdk-interacting protein Cip1 is a potent inhibitor of G1 cyclin-dependent kinases. *Cell*, **75**, 805–816.
16. el-Deiry, W.S., Tokino, T., Velculescu, V.E., Levy, D.B., Parsons, R., Trent, J.M., Lin, D., Mercer, W.E., Kinzler, K.W. and Vogelstein, B. (1993) WAF1, a potential mediator of p53 tumor suppression. *Cell*, **75**, 817–825.
17. Brugarolas, J., Chandrasekaran, C., Gordon, J.I., Beach, D., Jacks, T. and Hannon, G.J. (1995) Radiation-induced cell cycle arrest compromised by p21 deficiency. *Nature*, **377**, 552–557.
18. Deng, C., Zhang, P., Harper, J.W., Elledge, S.J. and Leder, P. (1995) Mice lacking p21CIP1/WAF1 undergo normal development, but are defective in G1 checkpoint control. *Cell*, **82**, 675–684.
19. Sheikh, M.S., Rochefort, H. and Garcia, M. (1995) Overexpression of p21WAF1/CIP1 induces growth arrest, giant cell formation and apoptosis in human breast carcinoma cell lines. *Oncogene*, **11**, 1899–1905.
20. Ornitz, D.M. and Leder, P. (1992) Ligand specificity and heparin dependence of fibroblast growth factor receptors 1 and 3. *J. Biol. Chem.*, **267**, 16305–16311.
21. Yang, X., Li, C., Xu, X. and Deng, C. (1998) The tumor suppressor SMAD4/DPC4 is essential for epiblast proliferation and mesoderm induction in mice. *Proc. Natl Acad. Sci. USA*, **95**, 3667–3672.
22. Lakso, M., Pichel, J.G., Gorman, J.R., Sauer, B., Okamoto, Y., Lee, E., Alt, F.W. and Westphal, H. (1996) Efficient *in vivo* manipulation of mouse genomic sequences at the zygote stage. *Proc. Natl Acad. Sci. USA*, **93**, 5860–5865.
23. Schindler, C., Shuai, K., Prezioso, V.R. and Darnell, J.E. Jr (1992) Interferon-dependent tyrosine phosphorylation of a latent cytoplasmic transcription factor. *Science*, **257**, 809–813.
24. Fu, X.Y. and Zhang, J.J. (1993) Transcription factor p91 interacts with the epidermal growth factor receptor and mediates activation of the c-fos gene promoter. *Cell*, **74**, 1135–1145.
25. Delezoide, A.L., Lasselin-Benoist, C., Legeai-Mallet, L., Brice, P., Senee, V., Yayon, A., Munnich, A., Vekemans, M. and Bonaventure, J. (1997) Abnormal FGFR 3 expression in cartilage of thanatophoric dysplasia fetuses. *Hum. Mol. Genet.*, **6**, 1899–1906.
26. Horton, W.A. (1997) Fibroblast growth factor receptor 3 and the human chondrodysplasias. *Curr. Opin. Pediatr.*, **9**, 437–442.
27. Muenke, M. and Schell, U. (1995) Fibroblast-growth-factor receptor mutations in human skeletal disorders. *Trends Genet.*, **11**, 308–313.
28. Mulvihill, J.J. (1995) Craniofacial syndromes: no such thing as a single gene disease. *Nature Genet.*, **9**, 101–103. [Erratum. *Nature Genet.* (1995) **9**, 451.]
29. Lewanda, A.F., Meyers, G.A. and Jabs, E.W. (1996) Craniosynostosis and skeletal dysplasias: fibroblast growth factor receptor defects. *Proc. Assoc. Am. Physicians*, **108**, 19–24.
30. Webster, M.K. and Donoghue, D.J. (1997) FGFR activation in skeletal disorders: too much of a good thing. *Trends Genet.*, **13**, 178–182.
31. Arman, E., Haffner-Krausz, R., Chen, Y., Heath, J.K. and Lonai, P. (1998) Targeted disruption of fibroblast growth factor (FGF) receptor 2 suggests a role for FGF signaling in pregastrulation mammalian development. *Proc. Natl Acad. Sci. USA*, **95**, 5082–5087.
32. Deng, C., Bedford, M., Li, C., Xu, X., Yang, X., Dunmore, J. and Leder, P. (1997) Fibroblast growth factor receptor-1 (FGFR-1) is essential for normal neural tube and limb development. *Dev. Biol.*, **185**, 42–54.
33. Deng, C.X., Wynshaw-Boris, A., Shen, M.M., Daugherty, C., Ornitz, D.M. and Leder, P. (1994) Murine FGFR-1 is required for early postimplantation growth and axial organization. *Genes Dev.*, **8**, 3045–3057.
34. Xu, X., Weinstein, M., Li, C., Naski, M., Cohen, R.I., Ornitz, D.M., Leder, P. and Deng, C. (1998) Fibroblast growth factor receptor 2 (FGFR2)-mediated reciprocal regulation loop between FGF8 and FGF10 is essential for limb induction. *Development*, **125**, 753–765.
35. Yamaguchi, T.P., Harpal, K., Henkemeyer, M. and Rossant, J. (1994) fgfr-1 is required for embryonic growth and mesodermal patterning during mouse gastrulation. *Genes Dev.*, **8**, 3032–3044.
36. Bellus, G.A., McIntosh, I., Szabo, J., Aylsworth, A., Kaitila, I. and Francomano, C.A. (1996) Hypochondroplasia: molecular analysis of the fibroblast growth factor receptor 3 gene. *Ann. NY Acad. Sci.*, **785**, 182–187.
37. Hecht, J.T., Francomano, C.A., Horton, W.A. and Annegers, J.F. (1987) Mortality in achondroplasia. *Am. J. Hum. Genet.*, **41**, 454–464.
38. McKusick, V.A., Kelly, T.E. and Dorst, J.P. (1973) Observations suggesting allelism of the achondroplasia and hypochondroplasia genes. *J. Med. Genet.*, **10**, 11–16.
39. van der Geer, P., Hunter, T. and Lindberg, R.A. (1994) Receptor protein-tyrosine kinases and their signal transduction pathways. *Ann. Rev. Cell. Biol.*, **10**, 251–337.
40. Reimold, A.M., Grusby, M.J., Kosaras, B., Fries, J.W., Mori, R., Maniwa, S., Clauss, I.M., Collins, T., Sidman, R.L., Glimcher, M.J. and Glimcher, L.H. (1996) Chondrodysplasia and neurological abnormalities in ATF-2-deficient mice. *Nature*, **379**, 262–265.
41. Karaplis, A.C., Luz, A., Glowacki, J., Bronson, R.T., Tybulewicz, V.L., Kronenberg, H.M. and Mulligan, R.C. (1994) Lethal skeletal dysplasia from targeted disruption of the parathyroid hormone-related peptide gene. *Genes Dev.*, **8**, 277–289.
42. Weir, E.C., Philbrick, W.M., Amling, M., Neff, L.A., Baron, R. and Broadus, A.E. (1996) Targeted overexpression of parathyroid hormone-related peptide in chondrocytes causes chondrodysplasia and delayed endochondral bone formation. *Proc. Natl Acad. Sci. USA*, **93**, 10240–10245.
43. Karaplis, A.C. and Vautour, L. (1997) Parathyroid hormone-related peptide and the parathyroid hormone/parathyroid hormone-related peptide receptor in skeletal development. *Curr. Opin. Nephrol. Hypertension*, **6**, 308–313.

44. Amizuka, N., Warshawsky, H., Henderson, J.E., Goltzman, D. and Karaplis, A.C. (1994) Parathyroid hormone-related peptide-depleted mice show abnormal epiphyseal cartilage development and altered endochondral bone formation. *J. Cell. Biol.*, **126**, 1611–1623.
45. Vortkamp, A., Lee, K., Lanske, B., Segre, G.V., Kronenberg, H.M. and Tabin, C.J. (1996) Regulation of rate of cartilage differentiation by Indian hedgehog and PTH-related protein. *Science*, **273**, 613–622.
46. Legeai-Mallet, L., Benoist-Lasselin, C., Delezoide, A.L., Munnich, A. and Bonaventure, J. (1998) Fibroblast growth factor receptor 3 mutations promote apoptosis but do not alter chondrocyte proliferation in thanatophoric dysplasia. *J. Biol. Chem.*, **273**, 13007–13014.
47. Perez-Castro, A.V., Wilson, J. and Altherr, M.R. (1995) Genomic organization of the mouse fibroblast growth factor receptor 3 (Fgfr3) gene. *Genomics*, **30**, 157–162.
48. McLeod, M.J. (1980) Differential staining of cartilage and bone in whole mouse fetuses by alcian blue and alizarin red S. *Teratology*, **22**, 299–301.
49. Franklin, D.S. and Xiong, Y. (1996) Induction of p18INK4c and its predominant association with CDK4 and CDK6 during myogenic differentiation. *Mol. Biol. Cell*, **7**, 1587–1599.